J|A|C|S
COMMUNICATIONS

Published on Web 08/28/2004

Shape-Controlled Synthesis and Shape-Induced Texture of $MnFe_2O_4$ Nanoparticles

Hao Zeng,[†] Philip M. Rice,[‡] Shan X. Wang,[§] and Shouheng Sun*,[†]

IBM T. J. Watson Research Center, Yorktown Heights, New York 10598, IBM Almaden Research Center, 650 Harry Road, San Jose, California 95120, and Department of Materials Science and Engineering, Stanford University, Stanford, California 94305

Received July 8, 2004; E-mail: ssun@us.ibm.com

The shape is one of the most important factors in determining the structural, physical, and chemical properties of a nanoparticle and an assembled array of the particles.[1] Shape-controlled synthesis of nanoparticles has become a recent focus, as different shapes of the particles can introduce electronic, optical, and magnetic properties that are different from those observed in their spherical counterparts. Semiconductor nanoparticles have been made in various nonspherical shapes of triangle, rod, cube, arrow, and tetrapod,[2] which are interesting for quantum confinement studies and important for potential sensor, transistor, and solar cell applications. As the restoring force on the conduction electrons is extraordinarily sensitive to particle curvature, nonspherical metallic Au or Ag nanoparticles, produced via various approaches,[3] have been found to shift their surface plasmon frequency drastically,[4] making them useful as multicolor diagnostic labels and for other optical devices. Controlling the shape of a magnetic nanoparticle is even more appealing as the shape may lead to anisotropic magnetic properties of the nanoparticles.[5] Although recent progress in shape-controlled synthesis of magnetic nanoparticles has led to nanorods,[6] nanocubes,[7] and other variously shaped Fe_2O_3 nanoparticles,[8] there is still no example of using nanoparticles with different shapes as building blocks to control the crystal orientation of the nanoparticles in an assembly. As the magnetic easy axis of a particle correlates closely with its crystal structure,[9] the shape-induced crystal orientation of each nanoparticle in an assembly would lead to an aligned magnetic easy axis. Such alignment is often a necessity for a nanoparticle assembly to be suitable for various magnetic applications in such as data storage and advanced magnets.[10]

Here we report shape-controlled synthesis of $MnFe_2O_4$ nanoparticles and shape-induced texture of the particles in a self-assembled superlattice. We recently reported that reaction of $Fe(acac)_3$ and $M(acac)_2$ with 1,2-hexadecanediol, oleic acid, and oleylamine in a high-boiling ether solvent could lead to monodisperse MFe_2O_4 nanoparticles (M = Fe, Co, Mn, Mg, etc.). The composition of the particles was controlled by the initial molar ratio of $Fe(acac)_3$ and $M(acac)_2$, and the size was tuned by varying the reaction conditions or via seed-meditated growth.[11] Our further experiments indicated that the size of the MFe_2O_4 particles (M = Mn in this work) could be tuned more conveniently through a one-pot reaction by changing the concentration of the reactants. More importantly, this one-pot reaction could also lead to the particles with controlled shapes. Slow evaporation of the particle dispersion yielded nanoparticle superlattices. The nanoparticles within the superlattice exhibited preferred alignment of crystal orientations correlated with their shape. With this texture control, the shaped nanoparticles could become useful building blocks for the construction of functional nanostructures.

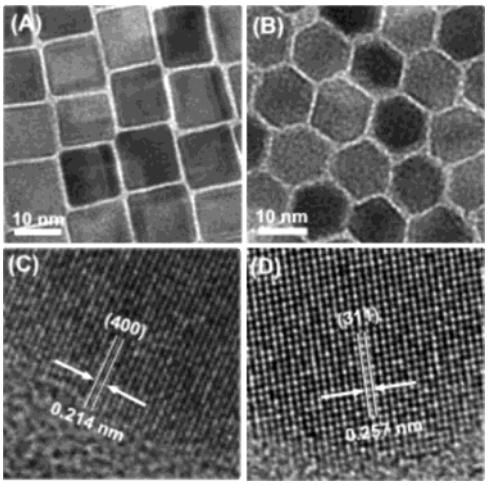

Figure 1. TEM images of the as synthesized (A) 12 nm cubelike and (B) 12 nm polyhedron-shaped $MnFe_2O_4$ nanoparticles. HRTEM images of a part of a single (C) cubelike and (D) polyhedron-shaped $MnFe_2O_4$ nanoparticles.

The size of the $MnFe_2O_4$ particles is tuned by varying the concentration of the precursors, while the shape is controlled by the amount of stabilizers added to the reaction mixture. For a reaction containing 2 mmol of $Fe(acac)_3$, 1 mmol of $Mn(acac)_2$, 10 mmol of 1,2-hexadecandiol, 6 mmol of oleic acid, 6 mmol of oleylamine, 20 mL of benzyl ether gave 12 nm $MnFe_2O_4$, while 22 mL or 25 mL of benzyl ether yielded 10- or 8 nm particles, respectively. When the surfactant/$Fe(acac)_3$ ratio is smaller than 3:1, the particles are nearly spherical with no well-defined facets.[12] Increasing the ratio to 3:1 yields cubelike particles.[13] If the particles were prepared using the seed-mediated growth as reported before,[11] polyhedron-shaped particles were obtained. Figure 1 shows the representative TEM images of the $MnFe_2O_4$ nanoparticles with different morphologies, with 1A being cubelike and 1B polyhedron-shaped particles. The HRTEM image of a part of a single cubelike $MnFe_2O_4$ nanoparticle (Figure 1C) shows lattice fringes with the interfringe distance measured to be 0.214 nm, and that of a polyhedron-shaped particle (Figure 1D) shows the interfringe distance to be 0.257 nm, close to the lattice spacing of the {400} planes at 0.213 nm and {311} planes at 0.256 nm in the cubic spinel-structured $MnFe_2O_4$. HRTEM further reveals that the {400} lattice fringes are parallel to the edges of the cube, while the {220} fringes (spacing 0.301 nm) run face-diagonally in the cube,[12] indicating that the cubelike particles are terminated with {100} planes. The TEM tilted angle analyses of the polyhedron-shaped particles indicated that the hexagon shape shown in Figure 1B likely

[†] IBM T. J. Watson Research Center.
[‡] IBM Almaden Research Center.
[§] Stanford University.

10.1021/ja045911d CCC: $27.50

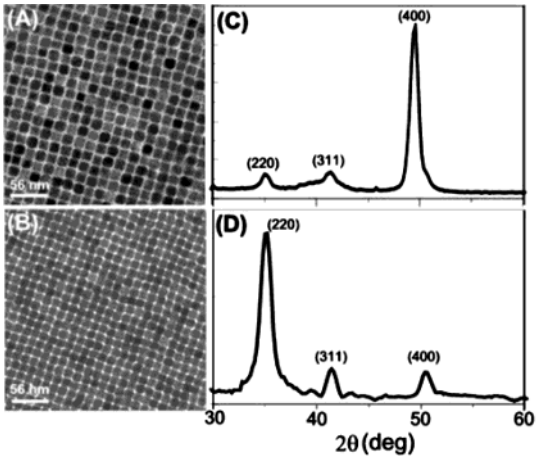

Figure 2. TEM images of 12 nm $MnFe_2O_4$ nanoparticle superlattices of (A) cubelike and (B) polyhedron-shaped nanoparticles. XRD (Co Kα λ = 1.788965 Å) of (C) cubelike and (D) polyhedron-shaped nanoparticle superlattice on Si(100) substrates.

comes from a truncated dodecahedron projected along the ⟨110⟩ direction, an observation that is similar to that of polyhedron-shaped Fe_2O_3 nanoparticles reported previously.[8]

Controlled evaporation of the carrier solvent from hexane dispersion (~2 mg/mL) of the particles led to $MnFe_2O_4$ nanoparticle superlattices. Figure 2A shows the superlattice assembly from the cubelike particles, while Figure 2B is the assembly from the polyhedron-shaped particles. The fast Fourier transformation (FFT) of these two images reveals four-fold symmetry,[12] indicating that both assemblies have the cubic packing. Scanning electron microscopy (SEM) images of the self-assembled nanoparticle superlattices on Si (100) substrate show large-area superlattice patterns[12] similar to those shown in Figure 2A,B. Although the assembly structures are the same for both cubelike and polyhedron-shaped particles, the different shapes possessed by each group of the particles do affect the crystalline orientation of individual particles within the self-assembled superlattices. XRD of the self-assembled cubelike particles on Si (100) substrate shows the intensified (400) peak (Figure 2C), and that of polyhedron-shaped particles reveals two strong reflections from (220) (Figure 2D) and (440) planes (not shown here).[12] These are markedly different from that of a 3-D randomly oriented spinel-structured $MnFe_2O_4$ nanoparticle assembly, which shows a strong (311) peak.[12] The fact that the XRD of the cubelike particle assembly shows a strong (400) peak indicates that each of the cubelike particles in the cubic assembly has preferred crystal orientation with {100} planes parallel to the Si substrate. Selected area electron diffraction (SAED) on the assembly shown in Figure 2A reveals a single-crystal-like pattern,[12] indicating strong preferential alignment. The strongest reflections from {400} and {440} show four-fold modulation of the ring intensity, which is due to the coherent alignment of the individual particle's spinel lattice within the cubic superlattice. This means that the incident beam is parallel to the ⟨100⟩ orientation, further confirming the XRD observation shown in Figure 2C. Similarly, for the polyhedron-shaped particle assembly, both XRD in Figure 2D and SAED[12] indicate that the {110} planes are parallel to the substrate. These demonstrate clearly that particle shape can indeed induce texture in a self-assembled nanoparticle superlattice.

The present study on shape-controlled synthesis and shape-induced texture of $MnFe_2O_4$ nanoparticles offers a practical example that chemical process can be used to regulate the growth of a particle and control the crystal orientation of a particle in a superlattice assembly. Such capability of control will be significant in future fabrication of high-performance magnetic nanodevices. A robust magnetic nanoparticle superlattice array with an aligned magnetic easy axis and controlled magnetic interactions between the neighboring particles may revolutionize the information storage technology with unprecedented sensitivity and density.

Acknowledgment. The work was supported in part by DARPA/ONR under Grant No. N00014-01-1-0885.

Supporting Information Available: A typical experimental procedure for making 12 nm cubelike $MnFe_2O_4$ nanoparticles, and further characterization data for $MnFe_2O_4$ nanoparticles and their assemblies. This material is available free of charge via the Internet at http://pubs.acs.org.

References

(1) (a) Wang, Z. L. *Adv. Mater*. **1998**, *10*, 13−30. (b) Wang, Z. L. *J. Phys. Chem. B* **2000**, *104*, 1153−1175. (c) Wang, Z. L.; Dai, Z.; Sun, S. *Adv. Mater*. **2000**, *12*, 1944−1946. (d) Jana, N. R. *Angew. Chem., Int. Ed*. **2004**, *43*, 1536−1540. (e) Mohraz, A.; Moler, D. B.; Ziff, R. M.; Solomon, M. J. *Phys. Rev. Lett*. **2004**, *92*, 155503-(1−4). (f) Narayanan, R.; El-Sayed, M. A. *Nano Lett*. **2004**, *4*, 1343−1348.

(2) (a) Peng, X. G.; Manna, L.; Yang, W.; Wickham, J.; Scher, E.; Kadavanich, A.; Alivisatos, A. P. *Nature* **2000**, *404*, 59−61. (b) Manna, L.; Scher, E. C.; Alivisatos, A. P. *J. Am. Chem. Soc*. **2000**, *122*, 12700−12706. (c) Chen, C.-C.; Chao, C.-Y.; Lang, Z.-H. *Chem. Mater*. **2000**, *12*, 1516−1518. (d) Li, L.; Hu, J.; Yang, W.; Alivisatos, A. P. *Nano Lett*. **2001**, *1*, 349−351. (e) Pinna, N.; Weiss, K.; Urban, J.; Pileni, M.-P. *Adv. Mater*. **2001**, *13*, 261−264. (f) Jun, Y.-W.; Lee, S.-M.; Kang, N.-J.; Cheon, J. *J. Am. Chem. Soc*. **2001**, *123*, 5150−5151. (g) Jun, Y.-W.; Jung, Y.-Y.; Cheon, J. *J. Am. Chem. Soc*. **2002**, *124*, 615−619. (h) Huynh, W. U.; Dittmer, J. J.; Alivisatos, A. P. *Science* **2002**, *295*, 2425−2427. (i) Watt, A. A. R.; Meredith, P.; Riches, J. D.; Atkinson, S.; Rubinsztein-Dunlop, H. *Curr. Appl. Phys*. **2004**, *4*, 320−322.

(3) (a) Nikoobakht, B.; Wang, Z. L.; El-Sayed, M. A. *J. Phys. Chem. B* **2000**, *104*, 8635−8640. (b) Jin, R.; Cao, Y.; Mirkin, C. A.; Kelly, K. L.; Schatz, G. C.; Zheng, J. G. *Science*, **2001**, *294*, 1901−1903. (c) Jana, N. R.; Gearheart, L.; Murphy, C. J. *J. Phys. Chem. B* **2001**, *105*, 4065−4067. (d) Kim, F.; Song, J. H.; Yang, P. *J. Am. Chem. Soc*. **2002**, *124*, 14316−14317. (e) Sun, Y.; Xia, Y. *Science* **2002**, *298*, 2176−2179. (f) Jin, R.; Cao, Y. C.; Hao, E.; Mètraux, G. S.; Schatz, G. C.; Mirkin, C. A. *Nature* **2003**, *425*, 487−490. (g) Chen, S.; Wang, Z. L.; Ballto, J.; Foulger, S. H.; Carroll, D. L. *J. Am. Chem. Soc*. **2003**, 125, 16186−16187.

(4) (a) van der Zande, B. M. I.; Bohmer, M. R.; Fokkink, L. G. J.; Schonenberger, C. *J. Phys. Chem. B* **1997**, *101*, 852−854. (b) Yu, Y.-Y.; Chang, S.-S.; Lee, C.-L.; Wang, C. R. C. *J. Phys. Chem. B* 1997; 101, 6661−6664. (c) Sonnichsen, C.; Franzl, T.; Wilk, T.; von Plessen, G.; Feldmann, J.; Wilson, O.; Mulvaney, P. *Phys. Rev. Lett*. **2002**, *88*, 077402-(1−4).

(5) (a) Thurn-Albrecht, T.; Schotter, J.; Kastle, C. A.; Emley, N.; Shibauchi, T.; Krusin-Elbaum, L. Guarini, K.; Black, C. T.; Tuominen, M. T.; Russell, T. P. *Science* **2000**, *290*, 2126−2129. (b) Zeng, H.; Zheng, M.; Skomski, R.; Sellmyer, D. J.; Liu, Y.; Menon, L.; Bandyopadhyay, S. *J. Appl. Phys*. **2000**, *87*, 4718−4720.

(6) (a) Park, S.-J.; Kim, S.; Lee, S.; Khim, Z. G.; Xhar, K.; Hyeon, T. *J. Am. Chem. Soc*. **2000**, *122*, 8581−8582. (b) Puntes, V. F.; Krishnan, K. M.; Alivisatos, A. P. *Science* **2001**, *291*, 2115−2117.

(7) (a) Dumestre, F.; Chaudret, B.; Amiens, C.; Renaud, P.; Fejes, P. *Science* **2004**, *303*, 821−823. (b) Song, Q.; Zhang, Z. J. *J. Am. Chem. Soc*. **2004**, *126*, 6164−6168.

(8) Cheon, J.; Kang, N.-J.; Lee, S.-M.; Lee, J.-H.; Yoon, J.-H.; Oh, S. J. *J. Am. Chem. Soc*. **2004**, *126*, 1950−1951.

(9) Cullity, B. D. *Introduction to Magnetic Materials*; Addison-Wesley: Reading, Massachusetts, 1972; pp 207−247.

(10) (a) Sun, S.; Murray, C. B.; Weller, D.; Folks, L.; Moser, A. *Science* **2000**, *287*, 1989−1992. (b) Zeng, H.; Li, J.; Wang, Z. L.; Liu, J. P.; Sun, S. *Nature* **2002**, *420*, 395−398.

(11) (a) Sun, S.; Zeng, H. *J. Am. Chem. Soc*., **2002** *124*, 8204−8205. (b) Sun, S.; Zeng, H.; Robinson, D. B.; Raoux, S.; Rice, P. M.; Wang, S. X.; Li, G. *J. Am. Chem. Soc*. **2004** *126*, 273−279.

(12) See the Supporting Information.

(13) The growth conditions seem to be consistent with those from several recent observations that more surfactant facilitates thermodynamical growth of the particles. See, for example, refs 3e, 7b, and 8.

JA045911D